AIAA JOURNAL
Vol. 36, No. 4, April 1998

Vortex Breakdown on Pitching Delta Wing: Control by Intermittent Trailing-Edge Blowing

Peter V. Vorobieff*
Los Alamos National Laboratory, Los Alamos, New Mexico 87545
and
Donald O. Rockwell†
Lehigh University, Bethlehem, Pennsylvania 18015-3085

To retard the onset of vortex breakdown on a half-delta wing subjected to periodic, large-amplitude maneuvers to high angle of attack, controls were applied in the form of a deflectable flap at the leading edge and variable blowing at the trailing edge of the wing. Intermittent blowing, applied during the upstroke part of the pitching cycle, appears to be the most energetically efficient means of retarding the onset of breakdown. Corresponding values of a dimensionless blowing coefficient are an order of magnitude smaller than those traditionally employed. Particle image velocimetry measurements of the velocity field in the plane of the leading-edge vortex show that blowing-induced changes of the velocity field propagate upstream along the lower surface of the wing. Intermittent blowing produces a radical change in the velocity distribution near the surface of the delta wing that persists throughout the entire pitching cycle. The phase lag of the blowing-induced velocity appears to be central to maintaining retardation of the onset of breakdown.

Nomenclature

A_j = area of trailing-edge blowing nozzles
C = root chord of the delta wing
c_μ = dimensionless momentum blowing coefficient for constant blowing
Re = Reynolds number, $U_\infty C/$ kinematic viscosity
S = semispan of the delta wing
T = pitching period
t = time
U_∞ = freestream velocity
$\boldsymbol{v}$ = local velocity
v_j = trailing-edge blowing velocity
x = coordinate along the axis parallel to the lower surface of the wing, with origin at the apex
x_b = distance between the onset of breakdown and wing apex
α = angle of attack
$\bar{\alpha}$ = mean angle of attack
α_0 = pitching amplitude
β = leading-edge flap deflection from the neutral position
γ = angle between trailing-edge blowing direction and the centerline of the wing
Θ_μ = dimensionless momentum blowing coefficient for intermittent blowing
Λ = sweep angle of the delta wing
ω = azimuthal vorticity

Introduction

THE phenomenon of vortex breakdown on delta wings has been known and studied for nearly four decades, with the first reports of its observation belonging to Peckham and Atkinson.[1] In recent years, investigations have concentrated on the behavior of vortex breakdown on maneuvering delta wings, especially at high angles of attack.

Earlier experimental works on this topic, such as those of Reynolds and Abtahi,[2] Gilliam et al.,[3] and Wolffelt,[4] centered on tracking the onset of vortex breakdown and employed smoke and dye visualization techniques. In the more recent works of Magness et al.,[5] Lin and Rockwell,[6] and Cipolla and Rockwell,[7] emphasis was on characterizing quantitative aspects of the flowfield via particle image velocimetry (PIV). Comprehensive reviews of this approach are given by Adrian,[8] Rockwell et al.,[9,10] and Rockwell and Lin.[11] Increased interest in vortex breakdown on a maneuvering delta wing also inspired numerical simulations, such as those of Visbal.[12] Rockwell[13] and Visbal[14] provide overviews of vortex breakdown on a pitching delta wing from experimental and numerical points of view.

The issue of controlling the onset of vortex breakdown has also attracted the attention of researchers. Unsteady blowing–suction at the leading edge was applied to a stationary delta wing by Gu et al.[15] Helin and Watry[16] demonstrated the effectiveness of trailing-edge blowing on a delta wing. Ding and Shih[17] provided the first quantitative insight into the effect of trailing-edge blowing on a delta wing during a pitch-up maneuver.

To date, the possibility of optimizing the energetic efficiency of combined leading- and trailing-edge control has not been addressed. Our initial experiments[18] indicated that energy input from the applied controls can be significantly reduced by applying both intermittent leading- and trailing-edge flow actuation during the maneuver. The investigation of controlled vortex breakdown in the present study concentrates on understanding the physics of energetically efficient controls.

Experimental Apparatus and Parameters

The large-scale circulation water channel of the Fluid Mechanics Laboratories at Lehigh University was used for the experiments. The test section of the free-surface channel was made of transparent Plexiglas®. The length of the test section was 5.49 m, the width 0.62 m, and the depth 0.58 m. The water level was maintained at 0.53 m.

The model of the half-delta wing used in the experiments was made of Lexan. Schematics of the wing system are shown in Fig. 1. The wing was rigidly connected to a rotating disk mounted on a Plexiglas plate (false wall). The delta wing/false wall assembly could be mounted either vertically or horizontally. The false wall was used to isolate the flow past the half-delta wing from the actuating mechanisms, which were driven by four computer-controlled, high-resolution stepping motors. This system allowed variation of the angle of attack α, the deflection angle β (± 25 deg) of the leading-edge flap from the neutral position, the blowing angle γ, and the blowing velocity v_j. A detailed description of the actuating machinery

Received June 2, 1997; revision received Dec. 18, 1997; accepted for publication Dec. 22, 1997.

*Research Associate, Group DX-3/MST-10/CNLS, Mail Stop B258.
†Paul B. Reinhold Professor, Department of Mechanical Engineering. Member AIAA.

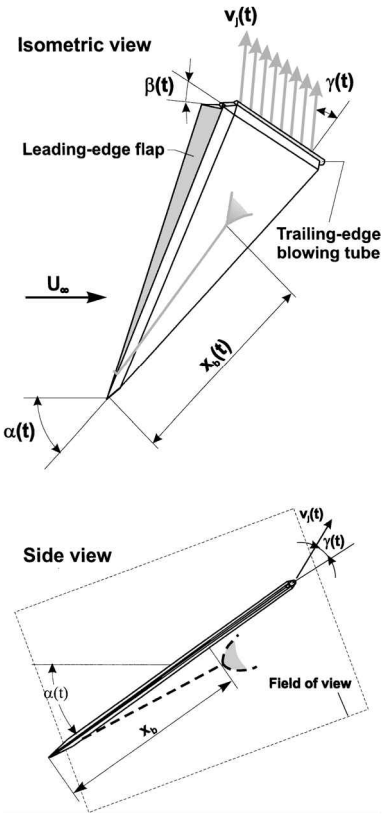

Fig. 1 Multiple-actuator half-delta wing schematics.

is given by Vorobieff and Rockwell.[18] The geometrical parameters of the delta wing were as follows: chord $C = 243$ mm, sweep angle Λ of the wing without the flap 75 deg and with the flap 72 deg, and wing thickness 12.7 mm. The parameters of the trailing-edge blowing tube used in the experiment were as follows: diameter 6.35 mm and orifice diameter 0.8 mm; the number of orifices was 37, giving a total area of the blowing orifices A_j equal to 18.3 mm^2. Trailing-edge blowing was laterally uniform within 20%.

The control experiments were conducted at a freestream velocity $U_\infty = 0.144$ m/s, corresponding to a Reynolds number $Re = 3.46 \times 10^4$ in terms of chord C. In all the experiments with pitching, the mean angle of attack $\bar{\alpha} = 40$ deg, the pitching amplitude $\alpha_0 = 10$ deg, and the pitching period $T = 2\pi/\omega = 10$ s, with sinusoidal pitching according to $\alpha(t) = \bar{\alpha} + \alpha_0 \sin \omega t$.

Acquisition of PIV Images

To investigate the physical mechanism underlying the energetic efficiency of trailing-edge blowing, high-image-density PIV was employed. Photographs of the global flow pattern were taken in the plane of the leading-edge vortex. Images were acquired at the rate of four frames per second during six successive pitching cycles, both with and without application of intermittent trailing-edge blowing. A Nikon F4 camera with a 105-mm lens was employed. It was tilted 27 deg from the horizontal to minimize the shadow region above the delta wing. The resulting field of view is shown in Fig. 1. The size of the image field for the photographs was 28×21 cm. In addition, PIV photographs of the flow in the trailing-edge region were taken with the horizontally oriented camera. The physical size of the image field was 8.5×6.4 cm. The shutter speed of the camera, selected to obtain four to five consecutive images of each particle per exposure, was $\frac{1}{125}$ s.

A bias mirror was placed in front of the camera lens at 45 deg to the optical axis of the camera to resolve directional ambiguity[19] by superimposing artificial uniform (bias) velocity on the flow. Zhang and Eisele[20] and Oschwald et al.[21] describe the possibility of distortions in the velocity field due to the influence of the bias mirror. To check for distortions, we compared a series of ensemble-averaged biased freestream PIV images with the series of images taken under the same conditions with the bias mirror deactivated. This comparison did not reveal any systematic distortions. In addition, we estimated the bias velocity distortion using the formulas of Oschwald et al.[21] and found it to be negligible, due to the extremely small angle of deflection of the bias mirror. For the photographs of the global flow pattern, the image field was sufficiently large to raise concerns about the limitations imposed on the accuracy of the PIV interrogation by the finite optical resolution of the system (undersampling errors), as described by Adrian.[22] Thus we followed the analysis procedure suggested by Adrian[22] to determine the error due to undersampling. It was also found to be negligible. Details of the image acquisition, validation, and interrogation procedures are described by Vorobieff.[23]

The location of the image plane was carefully selected after initial diagnostics. With the wing undergoing high angle-of-attack pitching motion, the angle between the core of the leading-edge vortex and the wall changes by as much as 3 deg. Thus it is impossible to maintain the laser sheet in perfect alignment with the core of the leading-edge vortex throughout the whole pitching cycle. The optimal laser sheet position was thus selected to maximize the time the sheet remains in alignment with the core. The duration of the interval of alignment within the pitching/control cycle was checked with dye injection into the leading-edge vortex. At different runs, alignment was changed to ensure that the combined PIV images with proper alignment cover the entire pitching cycle. With a thickness of the laser sheet on the order of 3 mm, this amounted to positioning it at an angle of 12 ± 1 deg to the false wall. In the present study, only images aligned with the core are employed. The onset of vortex breakdown in these images can be located by changes in the velocity/vorticity field indicating stagnation in the core of the vortex, with accuracy on the order of the grid size, corresponding to 1.4% of chord C.

Efficiency of Intermittent Trailing-Edge Blowing for Control of Vortex Breakdown

A combination of leading- and trailing-edge controls was sought to provide the most energetically efficient means of retarding vortex breakdown on the pitching wing. Some of the results are presented by Vorobieff and Rockwell[18]; a complete summary of control combinations is provided by Vorobieff.[23] Among the schemes examined were constant and intermittent trailing-edge blowing at various blowing angles and periodic deflections of the leading-edge flap. It was found that application of intermittent trailing-edge blowing during the upstroke part of the periodic pitching maneuver requires minimum energy input to produce a significant retardation of the onset of vortex breakdown. Figure 2 shows ensemble-averaged graphs of the distance x_b between the onset of vortex breakdown and the wing apex vs α. These results were obtained with dye visualization, with the error in locating the breakdown not exceeding 2 mm, or

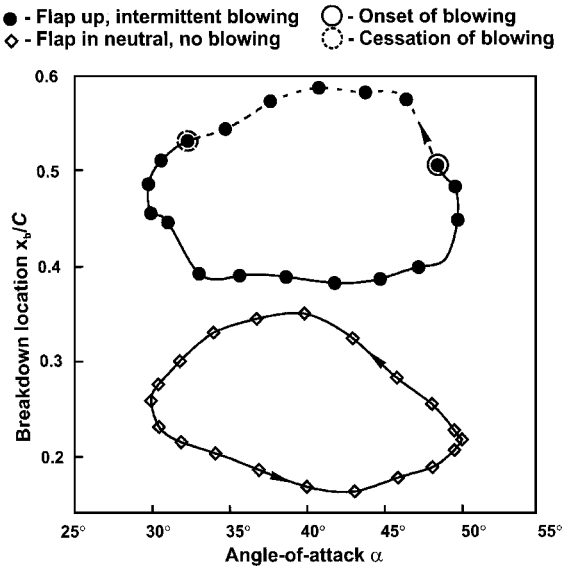

Fig. 2 Ensemble-averaged vortex breakdown location x_b vs angle of attack α for pitching with and without controls.

less than 1% of the chord length. To produce a considerable retardation of the onset of breakdown (with mean x_b increasing from $0.26C$ to $0.42C$), trailing-edge blowing with velocity $v_j = 4U_\infty$ was activated only for a duration of $0.4T$ during each pitching cycle. The traditional definition of the dimensionless momentum coefficient

$$c_\mu = \frac{(v_j/U_\infty)^2}{(A_j/S)^2}$$

is not adequate to describe the efficiency of blowing in the present case where the blowing velocity v_j is nonzero only during a fraction of the pitching cycle. Instead, we introduce a momentum coefficient that is time-averaged over one pitching/control application period:

$$\Theta_\mu = \left\{\left[\frac{1}{T}\int_0^T |v_j(t)|\,\mathrm{d}t\right]\Big/ U_\infty\right\}^2 \Big/ \left(\frac{A_j}{S}\right)^2$$

If the blowing has constant magnitude for all time, $\Theta_\mu = c_\mu$. The value of Θ_μ corresponding to the conditions described in Ref. 18 is 0.007. This value is substantially less than that typically employed in simulations of the effect of thrust vectoring on vortex breakdown. If, for example, continuous blowing is applied at a velocity $2U_\infty$ through an area corresponding to half of the cross section of the trailing edge of the wing, $c_\mu \approx 1.6$. This is close to the order of c_μ in the experiments of Ding and Shih[17] and Helin and Watry.[16] The blowing velocity in these experiments was also substantially higher, with values of $v_j = 7U_\infty$ employed by Ding and Shih[17] and v_j up to $8U_\infty$ by Helin and Watry.[16] The dimensionless momentum coefficient associated with intermittent blowing through small orifices at the trailing edge is therefore an order of magnitude smaller than that employed in related investigations.

This effectiveness of intermittent trailing-edge blowing can be augmented by deflection of a leading-edge flap at an angle $\beta = 25$ deg, measured upward from the neutral position; the consequence of this flap deflection is further retardation of vortex breakdown.[18] Moreover, the effect of stationary deflection of the flap over the pitching cycle has an effect closely resembling transient deployment of a deflected flap during only the upstroke part of the maneuver. On the basis of these observations, it was decided to employ the constant, stationary flap deflection $\beta = 25$ deg during the motion of the wing.

Overview of Alteration of the Flow Pattern at the Trailing Edge and Its Upstream Influence

The changes in the velocity and vorticity distributions due to trailing-edge blowing are evident in Fig. 3. The jet-like flow at the trailing edge changes both the orientation and the character of the flow downstream of the trailing edge. The case of no blowing is characterized by formation of a nearly stagnant zone at the base of the trailing edge and corresponding layers of positive and negative vorticity from the upper and lower edges of the trailing edge, respectively. The positive layer merges with the negative layer from the upper surface to form a mixing-layer flow. With jet blowing, the flow induced by entrainment tends to be aligned with the axis of the jet, precluding formation of a low-velocity region at the base. The jet exhibits pronounced concentrations of positive (solid line) and negative (dashed line) vorticity. Evaluation of the velocity magnitudes in the region immediately adjacent to the lower surface of the delta wing reveals a high velocity magnitude $\sim U_\infty$. Further evaluation of regions upstream of the image portion given in Fig. 3, to be addressed subsequently, indicates that this high velocity adjacent to the surface extends upstream to a distance of $C/2$ from the trailing edge. The local application of blowing therefore induces a global influence along a substantial extent of the wing surface.

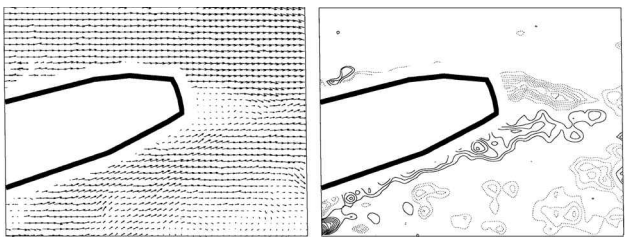

No blowing

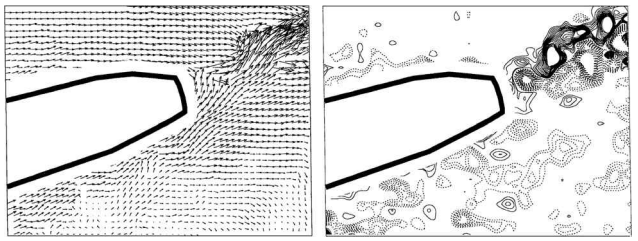

Blowing

Fig. 3 Influence of blowing on velocity and vorticity distributions near the trailing edge; α = 40 deg, upstroke: ——, positive vorticity contour, and – – –, negative vorticity contour.

Figures 4 and 5 compare the patterns of velocity and azimuthal vorticity on the delta wing for the cases with and without blowing. In each figure, the left and right columns of images correspond, respectively, to no blowing and blowing. Images in Fig. 4 were obtained at the beginning of the upstroke part of the pitching cycle ($\alpha = 30$ deg), whereas the images in Fig. 5 were acquired at the midportion of the upstroke ($\alpha = 40$ deg). Images on the left and right are phase matched.

Comparison of the overall flow patterns in the left and right columns of Figs. 4 and 5, especially those of the vorticity contours, shows that application of blowing results in retardation of the onset of breakdown and a substantial reduction of the width of the separated zone in the breakdown region. The location of the onset of breakdown throughout the pitching cycle (which can be identified either as the stalling point at the vortex core or the point where azimuthal vorticity concentrations surrounding the core change sign) is consistent with the dye-visualization measurements of x_b from previous research,[18] an excerpt of which is given in Fig. 2.

Detailed Comparison of Flow Patterns

Figure 4 shows the flow patterns at the beginning of the upstroke cycle ($\alpha = 30$ deg). This instant is immediately before activation of trailing-edge blowing; it occurs at a dimensionless time $t/T = 0.6$ after the cessation of blowing in the previous pitching and control cycle. Nevertheless, the increase of velocity magnitude under (on the leeward side of) the delta wing due to blowing is clearly evident all the way upstream to the onset of breakdown. For example, the maps of velocity magnitude $|\boldsymbol{v}|/U_\infty$ in Fig. 4 show that the velocity adjacent to the wing for the no-blowing case does not exceed $0.72U_\infty$. On the other hand, trailing-edge blowing accelerates the flow in this area to values slightly exceeding the freestream velocity U_∞.

The effect of blowing on the velocity distribution near the surface of the wing is even more prominent in Fig. 5, which represents the midupstroke cycle ($\alpha = 40$ deg) of the pitching maneuver, while trailing-edge blowing is active. Clearly visible is the high-velocity, jet-like flow near the trailing edge. The flow adjacent to the surface of the wing has values exceeding $1.4U_\infty$.

Ensemble-averaged velocity magnitude profiles under the delta wing are compared in Fig. 6. Six instantaneous PIV images were used for each of the averages. The graphs in the upper row show averaged data for the same angle of attack during the upstroke of the pitching cycle as addressed earlier, $\alpha = 30$ and 40 deg. The profiles on the left were taken at a location of approximately $\frac{2}{3}$ midchord, $x/C = 0.65$, whereas on the right they were taken immediately downstream of the trailing edge at $x/C = 1.05$.

At $\alpha = 30$ deg, the intermittent trailing-edge blowing has been inactive for 6 s, corresponding to a time delay $\Delta t/T = 0.6$. Nevertheless, the case of trailing-edge blowing exhibits a profile with much higher velocity near the wall at $\frac{2}{3}$ chord: $0.9U_\infty$ with blowing (solid line) vs $0.55U_\infty$ without blowing (dashed line). Downstream of the trailing edge, the zone of low velocity in the vicinity of the edge is present only for the case without blowing. The differences in velocity distribution at $\alpha = 40$ deg are even more dramatic. At two-thirds chord, the flow velocity near the wall increases from $0.7U_\infty$ to $1.25U_\infty$ due to blowing. For the case when intermittent

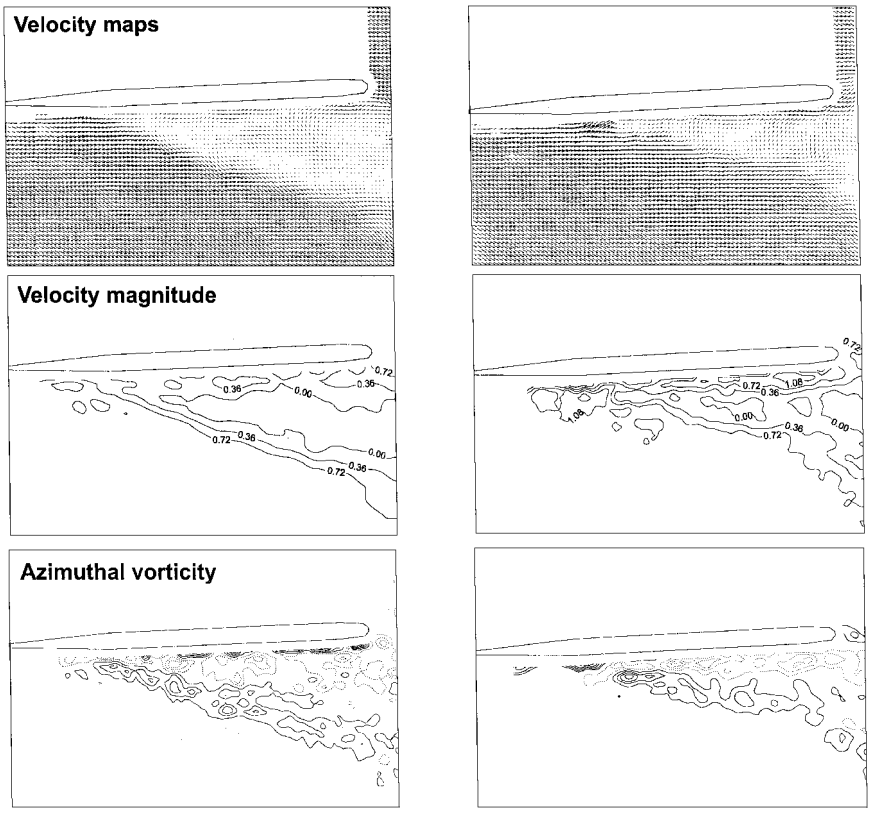

Fig. 4 Velocity and azimuthal vorticity for α = 30 deg, beginning of the upstroke. No blowing (left column) refers to absense of blowing during the entire pitching cycle. In the right column, blowing is actually applied only during the preceding portion of the cycle. At the instant shown, residual effects of blowing are evident due to phase lag.

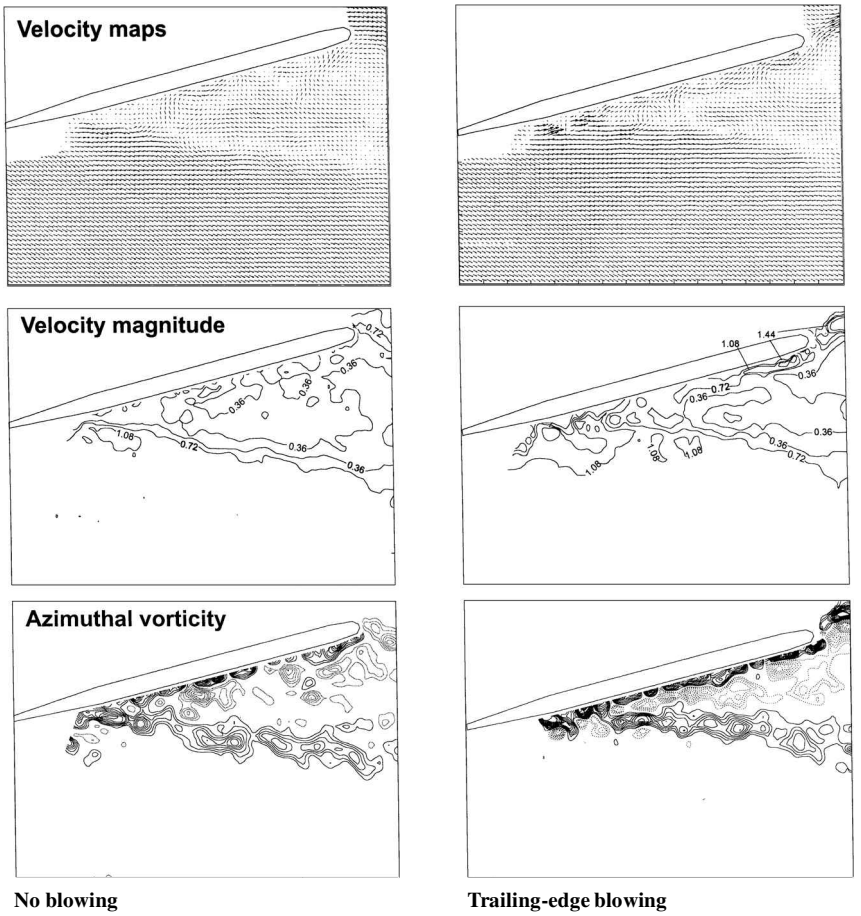

Fig. 5 Instantaneous velocity and azimuthal vorticity at α = 40 deg during the upstroke motion.

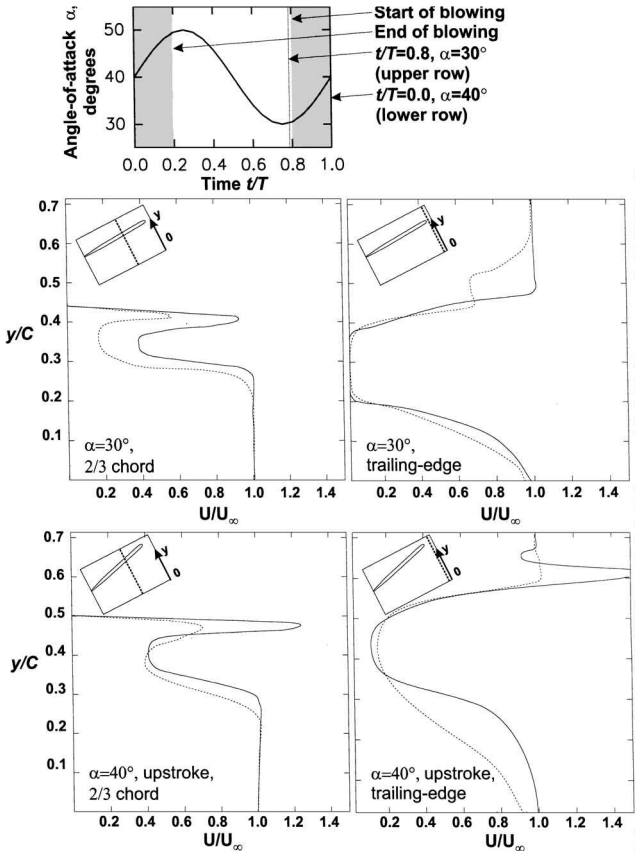

Fig. 6 Ensemble-averaged velocity magnitude profiles: – – –, no-blowing case, and ——, intermittent trailing-edge blowing. The sketch above the graphs shows the onset and cessation of blowing during the pitching cycle.

blowing is engaged, the trailing-edge velocity profile shows the presence of a sharply defined jet flow having a maximum velocity of approximately $4U_\infty$.

It is evident from the foregoing that the radical alteration of the velocity distribution near the lower surface of the wing, which extends farther upstream than midchord, directly influences the breakdown of the leading-edge vortex. This increase in the near-surface velocity apparently corresponds to a decrease in the magnitude of the adverse pressure gradient, which, in turn, causes retardation of the onset of breakdown.

Conclusions

The investigation of the influence of trailing-edge blowing on the location of vortex breakdown on a maneuvering delta wing shows that application of intermittent trailing-edge blowing during the upstroke part of the periodic pitching maneuver is the most energetically efficient way to retard the onset of vortex breakdown. The dimensionless momentum coefficient associated with this type of blowing is an order of magnitude smaller than that obtained in previous related studies, due to blowing intermittency and to considerable reduction in the area of the jet orifices.

The high efficiency of the intermittent trailing-edge blowing control mechanism is caused by the sensitivity of the onset of vortex breakdown to the time history of the flow and to the streamwise pressure gradient. A blowing-induced zone of high velocity exists far upstream from the trailing edge along the lower surface of the wing, thereby reducing the pressure gradient along the axis of the vortex. The effects of intermittent trailing-edge blowing persist throughout the entire pitching cycle, due to the phase lag of vortex breakdown relative to the pitching motion of the wing.

References

[1] Peckham, D. H., and Atkinson, S. A., "Preliminary Results of Low Speed Wind Tunnel Tests of a Gothic Wing of Aspect Ratio 1.0," Aeronautic Research Council, CP 508, 1957.

[2] Reynolds, G. A., and Abtahi, A. A., "Instabilities in Leading-Edge Vortex Development," AIAA Paper 87-2424, Aug. 1987.

[3] Gilliam, F., Wissler, J., and Robinson, M., "Visualization of Unsteady Separated Flow About a Pitching Delta Wing," AIAA Paper 87-0240, Jan. 1987.

[4] Wolffelt, K. W., "Investigation of the Movement of Vortex Burst Position with Dynamically Changing Angle of Attack for a Schematic Delta Wing in Water Tunnel with Correlation to Similar Studies in a Wind Tunnel," AGARD Conf. Proceedings, CP 413, 1986.

[5] Magness, C. M., Robinson, O., and Rockwell, D., "Control of Leading-Edge Vortices in a Delta Wing," AIAA Paper 89-0999, 1989.

[6] Lin, J.-C., and Rockwell, D., "Transient Structure of Vortex Breakdown on a Delta Wing," *AIAA Journal*, Vol. 33, No. 1, 1995, pp. 6–12.

[7] Cipolla, K. M., and Rockwell, D., "Flow Structure on Stalled Delta Wings Subjected to Small Amplitude Pitching Oscillations," *AIAA Journal*, Vol. 33, No. 7, 1995, pp. 1256–1262.

[8] Adrian, R. J., "Particle-Image Techniques for Experimental Flow Mechanics," *Annual Review of Fluid Mechanics*, Vol. 23, 1991, pp. 261–304.

[9] Rockwell, D., Magness, C., Robinson, O., Towfighi, J., Akin, O., Gu, W., and Corcoran, T., "Instantaneous Structure of Unsteady Separated Flows via Particle Image Velocimetry," Fluid Mechanics Labs., Lehigh Univ., Rept. PI-1, Bethlehem, PA, Feb. 1992.

[10] Rockwell, D., Magness, C., Robinson, O., Towfighi, J., Akin, O., and Corcoran, T., "High Image-Density Particle Image Velocimetry Using Scanning Techniques," *Experiments in Fluids*, Vol. 14, No. 3, 1993, pp. 181–192.

[11] Rockwell, D., and Lin, J.-C., "Quantitative Interpretation of Complex, Unsteady Flows via High Image-Density Particle Image Velocimetry," *SPIE Proceedings*, Vol. 2005, 1993, pp. 490–503.

[12] Visbal, M. R., "Numerical Simulation of Spiral Vortex Breakdown Above a Delta Wing," AIAA Paper 95-2309, June 1995.

[13] Rockwell, D., "Three-Dimensional Flow Structure on Delta Wings at High Angles-of-Attack: Experimental Concepts and Issues," AIAA Paper 93-0550, Jan. 1993.

[14] Visbal, M. R., "Structure of Vortex Breakdown on a Pitching Delta Wing," AIAA Paper 93-0434, Jan. 1993.

[15] Gu, W., Robinson, O., and Rockwell, D., "Control of Vortices on a Delta Wing by Leading-Edge Injection," *AIAA Journal*, Vol. 31, No. 7, 1993, pp. 1177–1185.

[16] Helin, H. E., and Watry, C. W., "Effects of Trailing-Edge Entrainment on Delta Wing Vortices," *AIAA Journal*, Vol. 32, No. 4, 1994, pp. 802–804.

[17] Ding, Z., and Shih, C., "Trailing-Edge Jet Control of the Leading-Edge Vortices of a Delta Wing," *AIAA Journal*, Vol. 34, No. 12, 1996, pp. 2642–2644.

[18] Vorobieff, P., and Rockwell, D., "Multiple-Actuator Control of Vortex Breakdown on a Pitching Delta Wing," *AIAA Journal*, Vol. 34, No. 10, 1996, pp. 2184–2186.

[19] Adrian, R. J., "Image Shifting Technique to Resolve Directional Ambiguity in Double-Pulsed Velocimetry," *Applied Optics*, Vol. 25, Nov. 1986, pp. 3855–3858.

[20] Zhang, Z., and Eisele, K., "The Two-Dimensional Velocity Shift Caused by the Use of a Rotating Mirror in PIV Flow Measurements," *Experiments in Fluids*, Vol. 20, No. 2, 1995, pp. 106–111.

[21] Oschwald, M., Bechle, S., and Welke, S., "Systematic Errors in PIV by Realizing Velocity Offsets with the Rotating Mirror Method," *Experiments in Fluids*, Vol. 18, No. 5, 1995, pp. 329–334.

[22] Adrian, R. J., "Limiting Resolution of Particle Image Velocimetry for Turbulent Flow," *Advances in Turbulence Research—1995*, 1995, pp. 1–19.

[23] Vorobieff, P. V., "Multiple-Actuator Control of Vortex Breakdown on a Maneuvering Delta Wing and Related Issues of Flow Analysis and Topology," Ph.D. Dissertation, Dept. of Mechanical Engineering and Mechanics, Lehigh Univ., Bethlehem, PA, 1996.

A. Plotkin
Associate Editor